Chemical Engineering Science 238 (2021) 116502

Contents lists available at ScienceDirect

Chemical Engineering Science

journal homepage: www.elsevier.com/locate/ces

Time scale analysis & characteristic times in microscale-based chemical and biochemical processes: Part I – Concepts and origins

Goran N. Jovanovic [a,*], Matthew Y. Coblyn [a], Igor Plazl [b]

[a] School of Chemical, Biological and Environmental Engineering, Oregon State University, Corvallis, OR 97331, USA
[b] Faculty of Chemistry and Chemical Technology, University of Ljubljana, Vecna Pot 113, 1000 Ljubljana, Slovenia

HIGHLIGHTS

- Time-Scale Analysis (TSA) is a novel engineering analysis & design approach.
- Characteristic Times are the fundamental elements of the TSA.
- TSA enables analysis of microscale-based reactors and unit operations.
- TSA facilitates analysis of microscale-based solid-catalyzed reaction process.

GRAPHICAL ABSTRACT

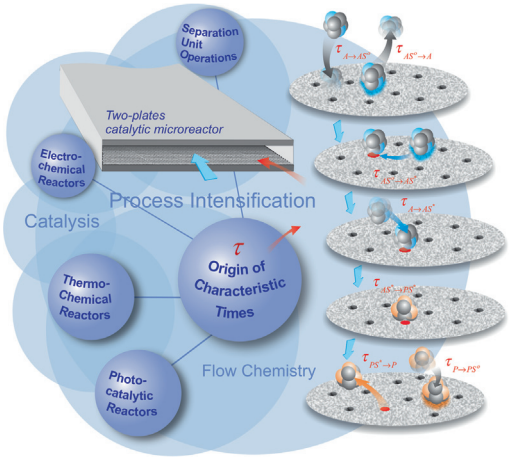

ARTICLE INFO

Article history:
Received 19 September 2020
Received in revised form 22 December 2020
Accepted 28 January 2021
Available online 8 February 2021

Keywords:
Time scale analysis
Characteristic times
Modeling-based design
Microscale-based technology

ABSTRACT

Time-Scale Analysis and *Characteristic Times* are suggested as a novel and useful tool in the analysis of the performance of microscale-based reactors, unit operations, and plant flow-sheet diagrams embodying microscale-based chemical processes. Transport phenomena, reaction kinetics, and phase contacting in microstructured architecture can be easily represented by unique time constants, $\tau_i[s]$. These Characteristic Times are estimated from first principles and are controlled by a user to support a meaningful chemical process analysis and provide insight or suggestions for successful design choices.

While the origin of Characteristic Times in microscale-based processes is rooted in fundamentals of molecular transport and reaction kinetics, the evolution of Characteristic Time definitions could be easily found in detailed mathematical models of microscale-based reaction processes and operations. The user-defined scaling parameters contribute to the flexibility of Time Scale Analysis implementation. This work uses a microscale-based solid catalyzed reaction process to demonstrate the concept of Time Scale Analysis and systematically define Characteristic Times and their origin. Lastly, varying forms of Time Scale Analysis have been implemented to evaluate specific phenomena or aspects of processes but have yet to encompass the full unit operation or process within the analysis. Part I and Part II of this work develop a comprehensive Time Scale Analysis for unit operations and a (bio)chemical process flowsheet (Part II only).

* Corresponding author.
E-mail address: goran.jovanovic@oregonstate.edu (G.N. Jovanovic).

https://doi.org/10.1016/j.ces.2021.116502
0009-2509/

Nomenclature

Latin symbols

A_n	Nominal wall surface coated by catalyst, $[m^2]$
a'	Catalyst surface per reactor volume, $[m^2_{cat}/m^2_r]$
a''	Catalyst surface per nominal reactor surface, $[m^2_{cat}/m^2_r]$
a_{S^o}	Normalized inactive catalyst surface, $\left[m^2_{S^o available}/m^2_{S^o total}\right]$
a_{S^*}	Normalized active catalyst surface, $[m^2_{S^* available}/m^2_{S^* total}]$
C_i	Concentration of species *i*, $[moli/m^3]$
C_A	Concentration of reactant *A*, $[mol\ A/m^3]$
$C_{A_{in}}$	Inlet concentration of reactant *A*, $[mol\ A/m^3]$
C_P	Concentration of species *P* (Eqs. (18)–(25)), $[mol\ P/m^3]$
C_{AS^o}	Surface concentration of species A^o_S (Eqs. (20)–(27)), $\left[mol\ A^o_S/m^2_{S^o}\right]$
C_{AS^*}	Surface concentration of species A^*_S (Eqs. (20)–(27)), $[molA^*_S/m^2_{S^*}]$
C_{PS^*}	Surface concentration of species P^*_S (Eqs. (20)–(27)), $[mol\ P^*_S/m^2_{S^*}]$
C_{PS^0}	Surface concentration of species P^o_S (Eqs. (20)–(27)), $\left[mol\ P^o_S/m^2_{S^o}\right]$
D	Diffusion coefficient, $[m^2/s]$
D_A	Diffusion coefficient of reactant *A*, $[m^2/s]$
F	Volumetric flow rate, $[m^3/s]$
h^{-1}	Probability of property displacement (Eq. (11)), $1/h \gg 0.5$
H	Halfway distance between reactor plates, $[m]$
$k_{A\rightarrow AS^o}$	Adsorption rate constant of species *A* to non-active sites (Eqs. (20)–(27)), $[1/s]$
$k_{AS^o\rightarrow A}$	Desorption rate constant of species *A* from non-active sites (Eqs. (20)–(27)), $[1/s]$
$k_{AS^o\rightarrow AS^*}$	Nominal surface diffusion rate constant (Eqs. (20)–(27)), $[1/s]$
$k_{A\rightarrow AS^*}$	Direct adsorption rate constant of species *A* to active cites (Eqs. (20)–(27)), $[1/s]$
$k_{AS^*\rightarrow PS^*}$	Reaction rate constant (Eqs. (20)–(27)), $[1/s]$
$k_{PS^*\rightarrow P}$	Direct-desorption rate constant of species P^*_S (Eqs. (20)–(27)), $[1/s]$
$k_{P\rightarrow PS^o}$	Adsorption rate constant of species *P* (Eqs. (20)–(27)), $[1/s]$
$k_{PS^o\rightarrow P}$	Desorption rate constant of species P^o_S (Eqs. (20)–(27)), $[1/s]$
L	Reactor length, $[m]$
k''	Reaction rate constant based on catalyst surface, $[m^3_r/m^2_{cat}\cdot s]$
p_k	Kinematic pressure, $[m^2/s^2]$
$-r''_A$	Reaction rate based on catalyst surface, $[mol/m^2_{cat}\cdot s]$; $-r''_A = -\frac{1}{S_c}\frac{dN_A}{dt} = k''C_A$
$\overrightarrow{s}_i$	i^{th}- single displacement step; *i = 1,2,3,...n* (Eqs. (3)–(8)), $[m]$
$\overrightarrow{s}^2$	Mean square value of single displacements (Eqs. (3)–(8)), $[m^2]$
$\overrightarrow{S}_n$	Vector sum of all single step displacements (Eqs. (3)–(8)), $[m]$
S^o	Catalyst surface containing non-active sites (Eqs. (20)–(27)), $\left[m^2_{S^o}\right]$
S^*	Catalyst surface containing active sites (Eqs. (20)–(27)), $\left[m^2_{S^*}\right]$
S_c	Total catalyst surface (Eqs. (20)–(27)), $[m^2_{cat}]$
$\bar{u}$	Average fluid velocity, $[m/s]$
$\overrightarrow{u}$	Velocity vector, $[m/s]$
u_x	*x* component of the velocity vector, $[m/s]$
V_r	Volume of reactor, $[m^3]$

Greek symbols

$\eta_{S^oAS^o}$	Surface of non-active sites on the catalyst, which is occupied with one mole of A^o_S adsorbed (Eqs. (20)–(27)), $\left[m^2_{S^o}/mol\ A^o_S\right]$
$\eta_{S^*AS^*}$	Surface of active sites on the catalyst, which is occupied with one mole of A^*_S adsorbed (Eqs. (20)–(27)), $[m^2_{S^*}/molA^*_S]$
$\eta_{S^oPS^o}$	Surface of non-active sites on the catalyst, which is occupied with one mole of P^o_S adsorbed (Eqs. (20)–(27)), $\left[m^2_{S^o}/mol\ P^o_S\right]$
$\eta_{S^*PS^*}$	Surface of active sites on the catalyst, which is occupied with one mole of P^*_S adsorbed (Eqs. (20)–(27)), $[m^2_{S^*}/mol\ P^*_S]$
λ^2	Square of the mean free path of molecules (Eqs. (8)–(11)), $[m^2]$
μ	Viscosity, $[Pa\cdot s]$
t_n	Mean time required for a single displacement step (Eqs. (7)–(9)), $[s]$
$\xi_{A\rightarrow AS^o}$	Stoichiometric conversion factor (Eqs. (20)–(27)), $\left[mol\ A^o_S/mol\ A\right]$
$\xi_{A\rightarrow AS^*}$	Stoichiometric conversion factor (Eqs. (20)–(27)), $[molA^*_S/molA]$
$\xi_{AS^o\rightarrow AS^*}$	Stoichiometric conversion factor (Eqs. (20)–(27)), $[molA^*_S/molA^o_S]$
$\xi_{AS^*\rightarrow PS^*}$	Stoichiometric conversion factor (Eqs. (20)–(27)), $[molP^*_S/molA^*_S]$
$\xi_{P\rightarrow PS^o}$	Stoichiometric conversion factor (Eqs. (20)–(27)), $[molP^o_S/molP]$
ρ	Property density (Eq. (11),11a), $[kg/m^3]$
ρ	Mass density, $[kg/m^3]$
τ_{diff}	Characteristic diffusion time, $[s]$
τ_i	Characteristic time, $[s]$
τ_{mrt}	Characteristic mean residence time, $[s]$
τ_r	Characteristic reaction time, $[s]$
$\tau_{A\rightarrow AS^o}$	Characteristic time of adsorption of the species onto the inactive catalyst surface (Eq. (18e)), $[s]$
$\tau_{AS^o\rightarrow A}$	Characteristic time of desorption of the species from the inactive catalyst surface (Eq. (18e)), $[s]$
$\tau_{A\rightarrow AS^*}$	Characteristic time of adsorption of the species onto the active catalyst surface (Eq. (18e)), $[s]$

1. Introduction

A substantial number of publications every year demonstrate how a microscale-based engineering approach can significantly improve reactant conversion, product selectivity, and shorten the time needed for chemical and biochemical transformations (Pohar and Plazl, 2009; Wegeng et al., 2000; Wohlgemuth et al., 2015; Yoshida et al., 2005). Similarly, the microscale-based reactor technologies demonstrate numerous advantages of microreactor devices such as superior rates of transport phenomena in chemical and biochemical reaction processes at controlled and repeatable conditions (Marques and Fernandes, 2011; Šalić and Zelić, 2018). New process design approaches such as continuous processing, flow chemistry, high-throughput screening, modularization, and

process intensification have emerged and opened novel pathways in process design and engineering (Bieringer et al., 2013; Gupta et al., 2010; Hunter et al., 2018; Kim et al., 2017; Miložič et al., 2017; Seifert et al., 2012). The aim of this contribution is in line with these technical approaches that enable smooth deployment of microscale-based technologies.

Time Scale Analysis (TSA) is an engineering analytical tool & design approach in which all processes, rates, fluxes, contact times, or any other dynamic phenomenon in an observed process are represented by their corresponding Characteristic Times. Characteristic Time is '*a time*', measured in seconds, that objectively represents the rate or intensity of any dynamic phenomenon in (bio)chemical process. The defining expressions, which enable exact calculation of the Characteristic Times are emerging from rigorous first principle based mathematical models of pertinent phenomena. Potential areas of implementation of Time Scale Analysis and Characteristic Times are graphically illustrated in Fig. 1. Generally, users of Time Scale Analysis are involved in the scaling of the mathematical model equations; thus, forming Characteristic Times, which enable meaningful chemical process analysis, provide insight into the operation of the process, and inform subsequent design choices. Previous authors have explored or utilized the concept of characteristic times and similar types of "scale analysis" in areas such as wastewater treatment, diffusion through layered media, combustion reactions, and exposure times for disinfection systems (Carr, 2018; Caudal et al., 2013; Henze et al., 2008; Isaac et al., 2013; Isvoranu et al., 2018; Lev and Regli, 1992; Wartha et al., 2020). Chavez and Debenedetti analyzed the process of supercritical antisolvent method, typically used for precipitation driven extraction, through estimation of the characteristic times for jet breakup, mass transfer, and nucleation (Chávez et al., 2003). Their findings pointed towards a diffusion-limited process where the jet breakup phenomenon occurs much faster than the mass transfer process. The authors noted the difficulty of estimating the characteristic time for nucleation due to its strong coupling with mass transfer through supersaturation and yet their approach to utilizing characteristic times provide significant insight into a complex and fast process. For applications in combustion, time scales within a system can vary across several orders of magnitude. Additionally, these processes can have massively complex sets of species and reactions which have led to significant work to develop solving methods including intrinsic low-dimensional manifold which prioritizes slow kinetics (Maas and Pope, 1992). In the biological realm, Klinke and Finley applied time scale analysis to a reaction rule-based model to assist in revealing the regulating steps in a biochemical signaling process (Klinke and Finley, 2012). Understanding flow time scale and characteristic chemical time scale can influence how multiscale flow-reaction models are implemented (Li et al., 2017) and a common dimensionless term utilized is the Damköhler number, relating chemical reaction and transport phenomena characteristic times (Fogler, 2006). Many of these dimensionless numbers that engineers are familiar with are based on characteristic times of the phenomena of interest.

This work looks to develop a wider definition of Characteristic Times and an approach to Time Scale Analysis that more fully encompasses chemical and biochemical processes.

In Part I of this work, we focus on the definition & origins of Characteristic Times. Formation of Characteristic Times is illustrated in a simple example of a solid-catalyzed chemical reaction process performed in a microscale-based reactor.

In Part II, a sequel paper, the Characteristic Times and Time Scale Analysis approach is illustrated to examine and suggest improvements in a biochemical reaction process. Additionally, in Part II, we demonstrate the application of TSA in the exploration of a process flow sheet diagram and the discovery of potential 'egresses' to process intensification.

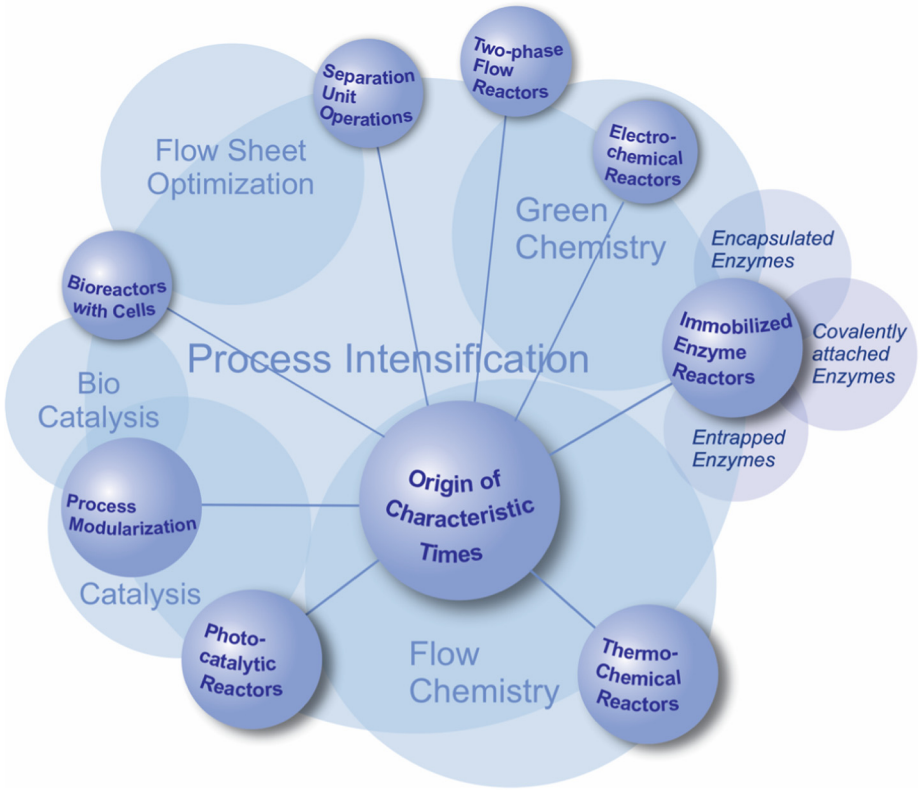

Fig. 1. Potential areas of implementation of the Time Scale Analysis and Characteristic Times.

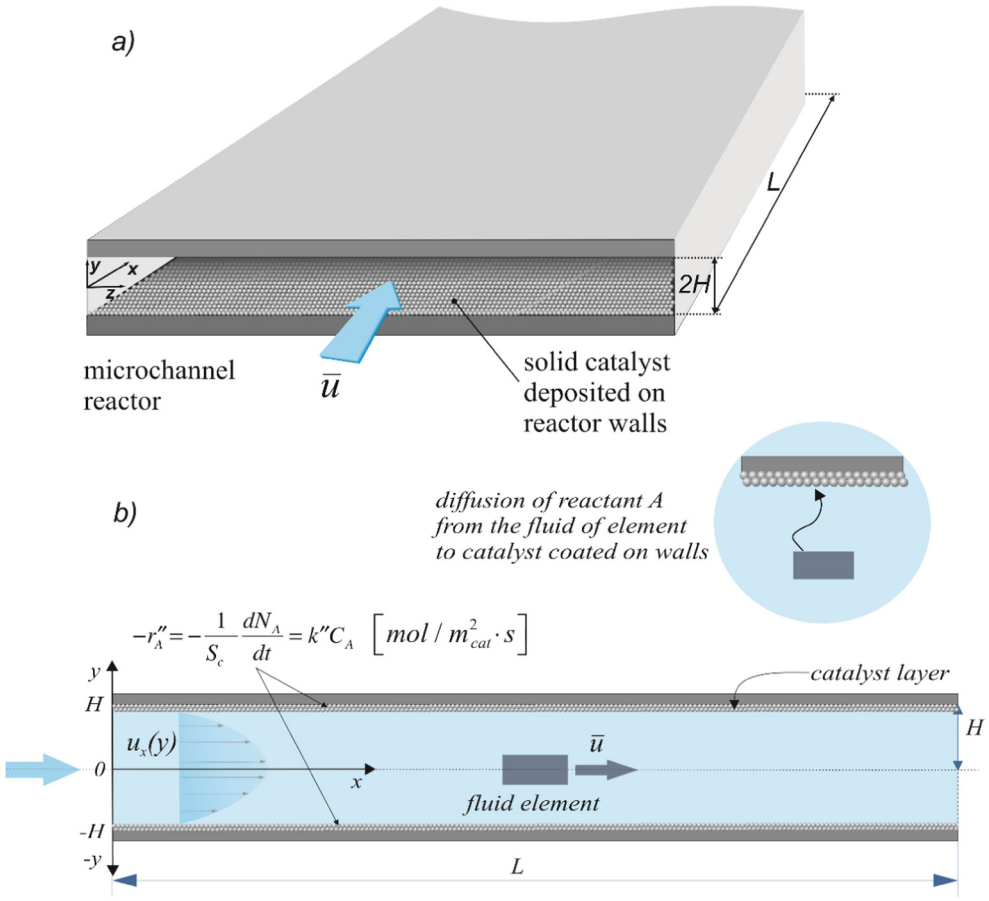

Fig. 2. Schematic representation of a microreactor designed between two parallel plates with solid catalyst deposited on reactor walls (a) and 2D physical domain of heterogeneous catalytic microreactor system (b).

2. The concept of characteristic times

Consider a simple microscale-based chemical reactor between two parallel plates coated with catalysts as shown in Fig. 2.

Notice that the fluid element is positioned approximately in the middle of the reactor between two catalyst-coated plates. It is evident that in this simplified representation of a microscale-based reactor, one could consider three characteristic times:

Mean Residence Time, τ_{mrt}, is an average time needed for the fluid element to be convectively transported from the entrance to the outlet of the reactor. The flow between plates is most probably laminar, which is a very reasonable assumption for flow characterization in microscale-based structures. Then, the centerline position of the fluid element shown in Fig. 2 will guarantee the shortest possible residence time of the element in the reactor. For the reaction process, this may not be the most favorable position. Any other position of the fluid element will be associated with a longer residence time in the reactor. In the time scale analysis, we may be more compelled to use the *mean residence time* of all fluid elements flowing through the reactor vessel.

Diffusion Time, τ_{diff}, is the time needed for a reactant species*A* to diffuse from the observed fluid element to the immediate vicinity of the coated catalyst at the reactor walls. Notice that the centerline position of the fluid element in the reactor is, again, not the most favorable position. The diffusion time of the reactant *A* from the centerline position to the reactor wall could be considered as the 'worst case' scenario.

Reaction Time, τ_r, is the time that can reasonably well represent the rate at which chemical reaction takes place. It is evident that chemical reactions are not infinitely fast; thus, it is useful to know how long it takes for a chemical reaction step(s) to take place. It is easy to anticipate that the characteristic reaction time must encompass a reaction rate constant. If a chemical reaction of interest represents the elemental step in the reaction kinetic scheme, then, the characteristic reaction time has more insightful meaning.

Therefore, for the reaction process schematically represented in Fig. 2, one could calculate the above-mentioned characteristic times if numerical values of process parameters and operating conditions are provided (Table 1a, 1b).

Based on the suggested numerical values in Table 1a, one can calculate characteristic times [19] as illustrated in Table 1b.

The order of magnitude of these characteristic times may be surprisingly small since they indeed appear to be several orders of magnitude smaller than corresponding times in macroscopic processes. Undeniably, microscale-based processes perform on much smaller spatial and temporal scales; at approximately 0.1 [mm] and 0.1 [s] respectively. Anticipations arising from a simple consideration of the best-desired performance of the process lead

Table 1a
Numerical values of assumed process parameters and operating conditions.

$k'' = 10^{-4}\,[m^3_{react}/m^2_{cat} \cdot s]$	Reaction rate constant based on catalyst surface;
$L = 0.01[m]$	Length of the reactor;
$H = 0.0001[m]$	Halfway distance between plates;
$\bar{u} = 0.01[m/s]$	Average fluid velocity;
$D_A = 10^{-6}\,[m^2/s]$	Diffusion coefficient of reactant *A*;
$S_c/V_r = 10^5\,[m^2_{cat}/m^3_r]$	Surface of catalyst to Volume of reactor ratio;

Table 1b
Numerical values of characteristic times.

$\tau_{mrt} = \frac{L}{u} = 1.0\ [s]$	Mean Residence Time
$\tau_r = \frac{V_r}{S_c}\frac{1}{k''} = 0.10\ [s]$	Reaction Time
$\tau_{diff} = \frac{H^2}{D_A} = 0.01\ [s]$	Diffusion Time

us to believe that the lineup of characteristic times should track the following relationship:

$$\tau_{mrt} > \tau_r \approx \tau_{diff} \tag{1}$$

Or, in words: mean residence time should be larger than the characteristic diffusion and reaction time, thus allowing several chances for the reactant *A* to diffuse to the proximity of the catalyst and react away at the catalyst surface. It is obvious that if $\tau_r > \tau_{diff}$ the process will be "*reaction-limited*"; while if $\tau_r < \tau_{diff}$ the process would be "mass-transfer" limited. Perhaps, a thoughtful design would require that $\tau_r \approx \tau_{diff}$. In any case, a somewhat longer τ_{mrt} would secure a higher conversion of reactant *A*.

It is interesting to note that adjustments of values of the characteristic times can be accomplished with relatively simple engineering actions. For example, to reduce the value of the characteristic reaction time shown in Table 1b, one could increase (S_c/V_r) ratio, by adding more catalyst surface (not necessarily more catalyst) or by simply increasing the operating temperature of the reactor, which will increase the reaction rate constant. Similarly, if τ_{mrt} is observed to be unnecessarily large, i.e., if a satisfactory conversion is reached much before the end of the reactor, one could increase the flow rate of the fluid, or reduce the length of the reactor.

However, a question may be raised as to the origins of the suggested simple algorithms for calculating the characteristic times. And, more importantly, we may be interested in defining a systematic way of creating other characteristic times, which could arise in a variety of different processes and areas of application (see Fig. 1).

$$\tau_{mrt} = \left(\frac{L}{u}\right) = \left(\frac{V_r}{F}\right);\ \tau_r = \left(\frac{V_r}{S_c}\frac{1}{k''}\right);\ \tau_{diff} = \left(\frac{H^2}{D_A}\right) \tag{2}$$

To illustrate the foundation of the approach in estimating the characteristic times, let us consider the characteristic diffusion time first.

3. Origins of characteristic times

From the kinetic theory of gases and the definition of Einstein random walk (Einstein, 1956), one can deduce the overall displacement ($\vec{S}_n$) of a molecule during a diffusion process. Overall displacement is the result of random steps such that $\vec{S}_n$ is the vector sum of all single step displacements, $\vec{s}_1,\ \vec{s}_2,\ \vec{s}_3,\ \vec{s}_1,\ \ldots\ \vec{s}_n$, as illustrated in Fig. 3.

$$\vec{S}_n = \vec{s}_1 + \vec{s}_2 + \vec{s}_3 + \ \ldots\ + \vec{s}_n \tag{3}$$

The square of the overall displacement vector $\vec{S}_n$ is represented by:

$$\begin{aligned}\left(\vec{S}_n\right)^2 &= \left(\vec{s}_1 + \vec{s}_2 + \vec{s}_3 + \ \ldots\ + \vec{s}_n\right)^2 \\ &= \vec{s}_1^{\,2} + \vec{s}_2^{\,2} + \vec{s}_3^{\,2} + \ \ldots\ + \vec{s}_n^{\,2} + 2\vec{s}_1\vec{s}_2 + 2\vec{s}_1\vec{s}_3 \\ &\quad + 2\vec{s}_1\vec{s}_4 + \ \ldots .\end{aligned} \tag{4}$$

Note that a sequence $\vec{s}_1,\ \vec{s}_2,\ \vec{s}_3,\ \vec{s}_1,\ \ldots\ \vec{s}_n$ is a sequence of random single-step displacement vectors, for which one can write:

$$\sum_{\substack{\forall\ n\ and\ p \\ where\ n \neq p}} \left(\vec{s}_n\right)^i \cdot \left(\vec{s}_{n+p}\right)^j = 0\ where\ i,j \in [1,n] \tag{5}$$

The above sum vanishes since there is no correlation between members of the random sequence. Therefore:

$$\begin{aligned}\left(\vec{S}_n\right)^2 &= \left(\vec{s}_1 + \vec{s}_2 + \vec{s}_3 + \ \ldots\ + \vec{s}_n\right)^2 \\ &= \vec{s}_1^{\,2} + \vec{s}_2^{\,2} + \vec{s}_3^{\,2} + \ \ldots\ + \vec{s}_n^{\,2} = \sum_{n=1}^{n} \vec{s}_n^{\,2}\end{aligned} \tag{4a}$$

If there is a quantity $\tilde{\vec{s}}^{\,2}$ such that:

$$\left(\vec{S}_n\right)^2 = \vec{s}_1^{\,2} + \vec{s}_2^{\,2} + \vec{s}_3^{\,2} + \ \ldots\ + \vec{s}_n^{\,2} = \sum_{n=1}^{n} \vec{s}_n^{\,2} = n \cdot \tilde{\vec{s}}^{\,2} \tag{4b}$$

then,

$$n = \frac{\left(\vec{S}_n\right)^2}{\tilde{\vec{s}}^{\,2}} \tag{6}$$

where $\tilde{\vec{s}}^{\,2}$ is the mean square value of a single displacement.

The time τ needed to complete n steps is proportional to n and $\bar{t}_n$, where $\bar{t}_n$ is the mean time required for the single displacement step, i.e.,

$$\tau \approx n\,\bar{t}_n \ \Rightarrow\ \tau \approx \frac{\left|\vec{S}_n\right|^2}{\left|\tilde{\vec{s}}^{\,2}\right|}\bar{t}_n \tag{7}$$

If the mean displacement $\left|\bar{S}_x\right|$ traveled by a molecule in the *x*-direction from its original position (as illustrated in Fig. 3) is proportional to $\left|\vec{S}_n\right|$, and if the mean square value of a single displacement $\left(\tilde{\vec{s}}^{\,2}\right)$ is the measure of the square of the mean free path of molecules (λ^2) experiencing random walk than one can write:

$$\tau \approx \frac{\left|\vec{S}_n\right|^2}{\left|\tilde{\vec{s}}^{\,2}\right|}\bar{t}_n \ \Rightarrow\ \tau = \frac{\left|\bar{S}_x\right|^2}{\left|\lambda^2\right|}\bar{t}_n \tag{8}$$

The quantity:

$$\frac{\lambda^2}{2\,\bar{t}_n} = D \tag{9}$$

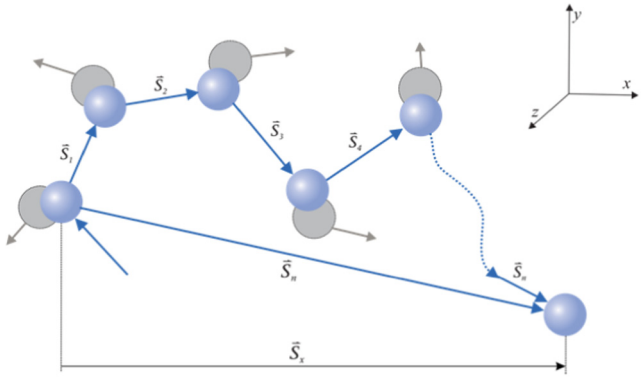

Fig. 3. Displacement by a sequence of random steps; Einstein random walk.

is defined as the diffusion coefficient, and the above expression represents its fundamental definition. Therefore, one can easily see that the time required for an observed mean displacement in the x-direction is given by:

$$\tau = \frac{\left|\bar{S}_x\right|^2}{2D} \tag{10}$$

which is very similar to the definition of the characteristic diffusion time used in Eq. (2).

$$\tau_{diff} = \frac{H^2}{D}$$

The development of the Fick Diffusion Equation in an isotropic gas leads to the expression:

$$\frac{\lambda^2}{h}\left[\left(\frac{\partial^2\rho}{\partial x^2}\right)+\left(\frac{\partial^2\rho}{\partial y^2}\right)+\left(\frac{\partial^2\rho}{\partial z^2}\right)\right] = \tau\left(\frac{\partial\rho}{\partial t}\right) \tag{11}$$

where ρ is the property (mass, ions, electrons, holes, ...) density subject to a random walk, and $1/h$ is the probability of the property displacement *sense* along the observed displacement orientation. For an ideal gas at low to normal pressures the probability $1/h \cong 0.5$, thus leading to:

$$\left(\frac{\lambda^2}{0.5\ \tau}\right)\left[\left(\frac{\partial^2\rho}{\partial x^2}\right)+\left(\frac{\partial^2\rho}{\partial y^2}\right)+\left(\frac{\partial^2\rho}{\partial z^2}\right)\right] = \left(\frac{\partial\rho}{\partial t}\right) \tag{11a}$$

where again, the diffusion coefficient D could be easily identified. The property density, ρ, in the Fick Diffusion Equation, can be replaced with mass density (concentration C_i) which leads to a familiar equation form:

$$D_i\frac{\partial^2 C_i}{\partial x^2}+D_i\frac{\partial^2 C_i}{\partial y^2}+D_i\frac{\partial^2 C_i}{\partial z^2}=\frac{\partial C_i}{\partial t} \tag{12}$$

The development of the *Fick Diffusion Equation* suggests that the characteristic diffusion time is organically embedded in the diffusion equation through the concept of the diffusion coefficient. Thus, a question arises if the *characteristic diffusion time* could be extracted back from the governing differential equation that represents the diffusion process. This is evidently possible and perhaps best demonstrated by considering a simple Parallel-Plate microscale-based chemical reactor coated with catalysts, as illustrated in Fig. 2. Mathematical model of the mass balance equation for this reactor (at steady state, unidirectional laminar flow, isothermal Newtonian fluid, and simple reaction kinetics that takes place at walls coated with catalyst) assumes the following form:

$$-u_x(y)\frac{\partial C_A(x,y)}{\partial x} + D_A\frac{\partial^2 C_A(x,y)}{\partial x^2}+D_A\frac{\partial^2 C_A(x,y)}{\partial y^2}=0 \tag{13}$$

where the velocity at any point in the reactor is determined by momentum balance equation (Navier-Stocks equations):

$$\frac{\Delta P}{L}-\mu\frac{\partial^2 u_x}{\partial y^2}=0 \tag{14}$$

with corresponding boundary conditions;

– for the mass balance equation:

$$@\ x=0\ C_A(0,y)=C_{Ain};\ @\ x=L\ \frac{\partial C_A(L,y)}{\partial x}=0 \tag{13a}$$

$$@y=0\ \frac{\partial C_A(x,0)}{\partial y}=0;\ @y=H\ -D\left.\frac{\partial C_A(x,y)}{\partial y}\right|_{y=H} = a''k''C_A|_{y=H} \tag{13b}$$

– for the momentum equation:

$$@\ y=0\ \frac{\partial u(x,0)}{\partial y}=0;\ \text{and}\ @\ y=H\ u(x,H)=0 \tag{14a}$$

One way to "extract" the characteristic times from the governing differential equation is to consider the *scaling* of dependent, (C_A), and independent variables, (x,y), in the mass balance equation. A reasonable suggestion for the scaling parameters is, $C_{Ain},\ L,\ H$.

Then, the new scaled variables could be represented as,

$$y^*=\frac{y}{H};\ x^*=\frac{x}{L};\ C_A^*=\frac{C_A}{C_{Ain}}\ \Rightarrow\ y=y^*H;\ x=x^*L;\ C_A=C_A^*C_{Ain} \tag{15a}$$

Similarly:

$$dy=H\cdot dy^*;\ dx=L\cdot dx^*;\ \partial C_A=C_{Ain}\partial C_A^* \tag{15b}$$

After substitutions of Equations (15a) and (15b) into the mass balance Equation (13) we obtain:

$$-1.5\cdot\frac{\bar{u}_x}{L}\left[1-(y^*)^2\right]\frac{\partial C_A^*}{\partial x^*}+\frac{D_A}{L^2}\frac{\partial^2 C_A^*}{\partial(x^*)^2}+\frac{D_A}{H^2}\frac{\partial^2 C_A^*}{\partial(y^*)^2}=0 \tag{16}$$

where $u_x(y)=1.5\cdot\bar{u}_x\left[1-\left(\frac{y}{H}\right)^2\right]$.

The coefficients in the normalized differential Equation (Eq. (16)) represent the characteristic times that are considered earlier:

$$-1.5\cdot\left(\frac{\bar{u}_x}{L}\right)\left[1-(y^*)^2\right]\frac{\partial C_A^*}{\partial x^*}+\left(\frac{D_A}{L^2}\right)\frac{\partial^2 C_A^*}{\partial(x^*)^2}+\left(\frac{D_A}{H^2}\right)\frac{\partial^2 C_A^*}{\partial(y^*)^2}=0 \tag{16a}$$

$$-1.5\frac{1}{\tau_{mrt}}\left[1-(y^*)^2\right]\frac{\partial C_A^*}{\partial x^*}+\frac{1}{\tau_{diff_x}}\frac{\partial^2 C_A^*}{\partial(x^*)^2}+\frac{1}{\tau_{diff_y}}\frac{\partial^2 C_A^*}{\partial(y^*)^2}=0 \tag{16b}$$

Similarly, the boundary conditions need to be scaled. Of particular interest is the scaling of the boundary condition at the surface of the catalyst.

$$@\ y=H\ -D_A\left.\frac{\partial C_A(x,y)}{\partial y}\right|_{y=H} = a''k''C_A|_{y=H} \tag{17}$$

$$@\ y^*=1\ -\frac{D_A}{H^2}\left.\frac{\partial C_A^*}{\partial y^*}\right|_{y^*=1} = \left(\frac{a''}{H}\right)k''C_A^*|_{y^*=1}\ \Rightarrow\ -\frac{D_A}{H^2}\frac{\partial C_A^*}{\partial y^*}=a'k''C_A^* \tag{17a}$$

$$\Rightarrow\ -\frac{D_A}{H^2}\frac{\partial C_A^*}{\partial y^*}=a'k''C_A^*,\ \text{where}\ a''(=)\frac{m_{cat}^2}{m_r^2}\ \text{and}\ a'(=)\frac{m_{cat}^2}{m_r^3} \tag{17b}$$

$$@\ y^*=1\ -\left(\frac{1}{\tau_{diff_y}}\right)\left.\frac{\partial C_A^*}{\partial y^*}\right|_{y^*=1} = \left(\frac{1}{\tau_r}\right)C_A^*|_{y^*=1} \tag{17c}$$

It is shown here by simple mathematical manipulation that the characteristic time constants emerge from the governing conservation equations. Because the characteristic times are indicative of the process step resistances a simple time scale analysis provides insight into the critical rate step such as the controlling step in the overall chemical reaction process rate. To illustrate this point, consider the boundary condition at the surface of the catalyst again. If,

$$\tau_{diff_y} >> \tau_r; \quad -\frac{1}{\tau_{diff_y}}\frac{\partial C_A^*}{\partial y^*}\bigg|_{y^*=1} = \frac{1}{\tau_r}C_A^*\bigg|_{y^*=1} \Rightarrow -\frac{\tau_r}{\tau_{diff_y}}^{\approx 0}\frac{\partial C_A^*}{\partial y^*} = C_A^* \Rightarrow \boxed{C_A^*\big|_{y^*=1} \cong 0}$$

$$\tau_{diff_y} << \tau_r; \quad -\frac{1}{\tau_{diff_y}}\frac{\partial C_A^*}{\partial y^*}\bigg|_{y^*=1} = \frac{1}{\tau_r}C_A^*\bigg|_{y^*=1} \Rightarrow -\frac{\partial C_A^*}{\partial y^*} = \frac{\tau_{diff_y}}{\tau_r}^{\approx 0} C_A^* \Rightarrow \boxed{\frac{\partial C_A^*}{\partial y^*} \cong 0}$$

It is now evident that the cases of *mass transfer limited process* and *reaction limited process* can be easily discriminated by observing the characteristic diffusion and characteristic reaction time. Moreover, TSA enables possible simplifications of model equations; and, thus, faster and easier modeling-based design. Numerically and computationally involved solutions may greatly benefit from the TSA analysis.

One should notice that the choice of scaling parameters for dependent and independent process variables is the most creative input that a user of TSA and Characteristic Times may contribute. The choice of scaling parameters reflects the level of intricacies and introspection into a (bio)chemical process operation that a user wants to achieve. The scaling parameters may often vary with space (position in the reactor) and time (in unsteady operations). In these cases, scaling parameters appear to have distributed values. Thus, one could ultimately consider the distribution of Characteristic Times in space and time. The user of the TSA & Characteristic Times must be aware of these possibilities and use them intelligently towards a greater understanding of (bio)chemical processes. In this paper, we will constrain the analysis using constant scaling parameters in all space and time domains. In Part II Appendix, we briefly discuss the appearance of distributed characteristic times as associated with Taylor flow.

4. Time scale analysis in solid catalyzed reaction process

It is interesting to employ the TSA concept in the analysis of the performance of a solid-catalyzed reaction process for which detailed microkinetic representation of the reaction kinetics is available. An important collateral benefit of the TSA in the identification of steps in the reaction process that need innovative improvements is the support of the concept of Process Intensification (Stankiewicz and Moulijn, 2000).

A simple case of a solid catalyzed reaction process is illustrated in Fig. 4.

One could assume that the following stoichiometric equations reflect the elemental events, including reaction kinetics steps, that take place on the surface of the catalyst.

One should note that species *A*(reactant) and species *P*(product) are the only species appearing in the bulk liquid flow. All other species are confined to the catalyst surface and never show in the bulk of the liquid. This is schematically illustrated in Fig. 5.

$A + (S^o) \underset{k_{AS^o\to A}}{\overset{k_{A\to AS^o}}{\rightleftharpoons}} A_S^o$	adsorption-desorption of A	(Fig. 4b)
$A_S^o + (S^*) \overset{k_{AS^o\to AS^*}}{\to} A_S^* + (S^o)$	activation of A_S^o	(Fig. 4c)
$A + (S^*) \overset{k_{A\to AS^*}}{\to} A_S^*$	direct activation of A	(Fig. 4d)
$A_S^* \overset{k_{AS^*\to PS^*}}{\to} P_S^*$	conversion of A_S^*	(Fig. 4e)
$P_S^* \overset{k_{PS^*\to P}}{\to} P + (S^*)$	direct desorption of P_S^*	(Fig. 4f)
$P + (S^o) \underset{k_{PS^o\to P}}{\overset{k_{P\to PS^o}}{\rightleftharpoons}} P_S^o$	adsorption-desorption of P	(Fig. 4f)

The above scheme of elemental steps is schematically illustrated in the Fig. 5.

The mathematical model of the mass balance for reactant *A* and product *P* that represents the steady state operation of a microscale-based reactor with solid catalyzed reaction process as shown schematically in Fig. 4 is given by Eqs. (18) and (19):

$$-u_x(y)\frac{\partial C_A}{\partial x} + D_A\frac{\partial^2 C_A}{\partial x^2} + D_A\frac{\partial^2 C_A}{\partial y^2} = 0 \quad \left[\frac{mol\ A}{m_r^3\cdot s}\right] \tag{18}$$

$$-u_x(y)\frac{\partial C_P}{\partial x} + D_P\frac{\partial^2 C_P}{\partial x^2} + D_P\frac{\partial^2 C_P}{\partial y^2} = 0 \quad \left[\frac{mol\ P}{m_r^3\cdot s}\right] \tag{19}$$

Mass balance Eqs. (18) and (19) need boundary conditions, which can be written for an apparently symmetric system of our main physical domain in the following form:

$$1:\ @y = 0\ \frac{\partial C_A}{\partial y}\Big|_{y=0} = 0;\ 2:\ @y = H\ -D_A A_n \frac{\partial C_A}{\partial y}\Big|_{y=H} = V_r(\Delta r_{C_A})$$
$$3:\ @x = 0\ C_A = C_{Ain};\ 4:\ @x = L\ \frac{\partial C_A}{\partial x}\Big|_{x=L} = 0 \tag{18a}$$

$$1:\ @y = 0\ \frac{\partial C_P}{\partial y}\Big|_{y=0} = 0;\ 2:\ @y = H\ -D_P A_n \frac{\partial C_P}{\partial y}\Big|_{y=H} = V_r(\Delta r_{C_P})$$
$$3:\ @x = 0\ C_P = 0;\ 4:\ @x = L\ \frac{\partial C_P}{\partial x}\Big|_{x=L} = 0 \tag{19a}$$

where Δr_{C_A} and Δr_{C_P} are the *net rate of change* of species *A* and *P*. It is now obvious that the entire kinetics will be introduced into the reaction process model through the boundary conditions of the (only) two species that appear in the bulk fluid of the reactor.

The proposed reaction kinetics, which is now following the elementary stoichiometric reaction steps on the surface of the catalyst (as schematically shown in Figs. 4 and 5), assumes the following *net rate of change* forms for each species:

$$\Delta r_{C_A} = -k_{A\to AS^o}C_A a_{S^o} + k_{AS^o\to A}C_{AS^o}\left(\frac{S^o}{V_r}\right)\xi_{A\to AS^o} - k_{A\to AS^*}C_A a_{S^*} \quad \left[\frac{mol\ A}{m_r^3\cdot s}\right] \tag{20}$$

$$\Delta r_{C_{AS^o}} = k_{A\to AS^o}C_A a_{S^o}\left(\frac{V_r}{S_c}\right)\xi_{A\to AS^o} - k_{AS^o\to A}C_{AS^o} - k_{AS^o\to AS^*}C_{AS^o}a_{S^*} \quad \left[\frac{mol\ A_S^o}{m_{S^o}^2\cdot s}\right] \tag{21}$$

$$\Delta r_{C_{AS^*}} = k_{AS^o\to AS^*}C_{AS^o}a_{S^*}\left(\frac{S^o}{S^*}\right)\xi_{AS^o\to AS^*} + k_{AS^o\to AS^*}C_A a_{S^*}\left(\frac{V_r}{S^*}\right)\xi_{A\to AS^*} - -k_{AS^*\to PS^*}C_{AS^*} \quad \left[\frac{mol\ A_S^*}{m_{S^*}^2\cdot s}\right] \tag{22}$$

$$\Delta r_{C_{PS^*}} = k_{AS^*\to PS^*}C_{AS^*}\xi_{AS^*\to PS^*} - k_{PS^*\to P}C_{PS^*} \quad \left[\frac{mol\ P_S^*}{m_{S^*}^2\cdot s}\right] \tag{23}$$

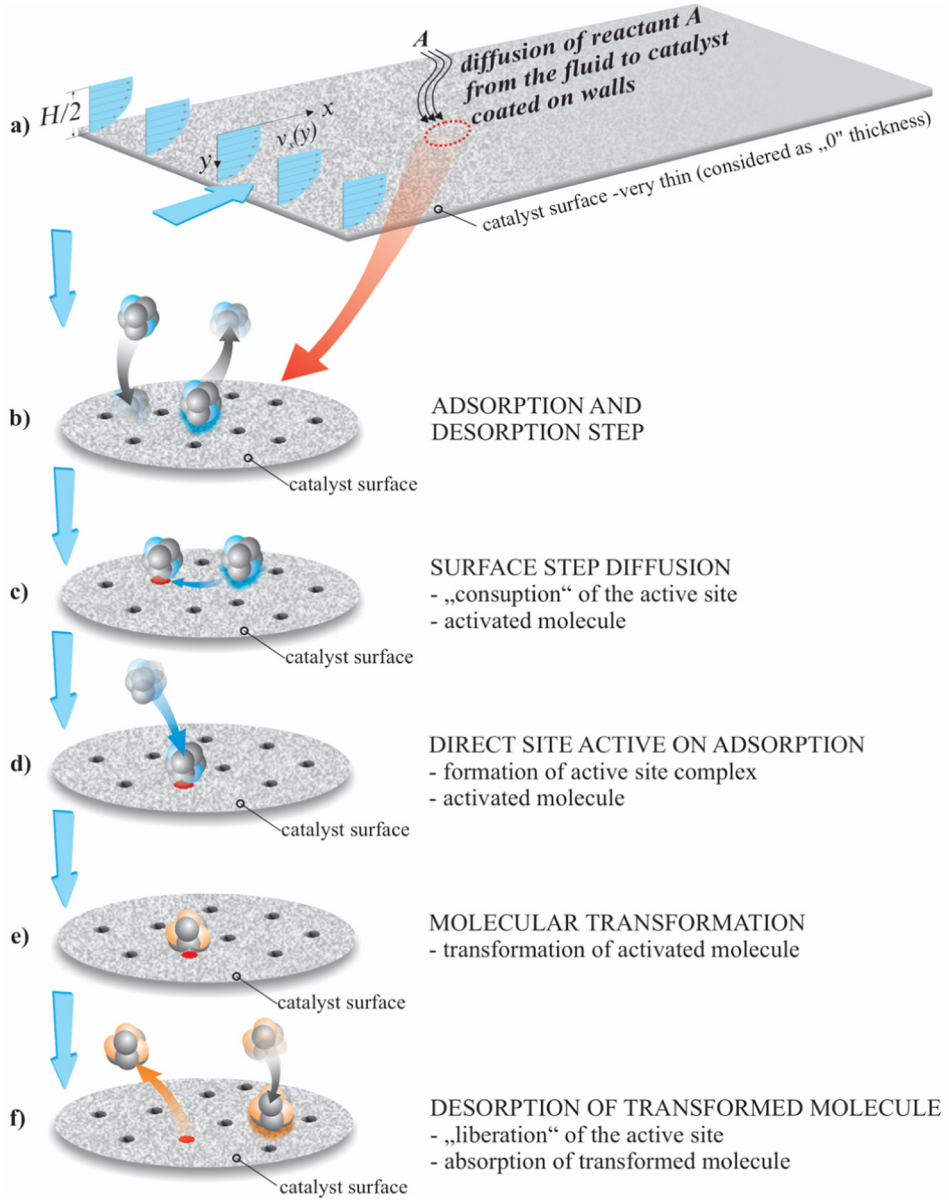

Fig. 4. Proposed schematic representation of a solid catalyzed reaction process.

$$\Delta r_{C_P} = k_{PS^* \to P} C_{PS^*} \left(\frac{S^*}{V_r}\right) - k_{P \to PS^o} C_P a_{S^o} + k_{PS^o \to P} C_{PS^o} \left(\frac{S^o}{V_r}\right) \xi_{PS^o \to P} \qquad \left[\frac{mol\ P}{m_r^3 \cdot s}\right] \tag{24}$$

$$\Delta r_{C_{PS^o}} = k_{P \to PS^o} C_P a_{S^o} \left(\frac{V_r}{S^o}\right) \xi_{P \to PS^o} - k_{PS \to P} C_{PS^o} \qquad \left[\frac{molP_S^o}{m_{S^o}^2 s}\right] \tag{25}$$

$$\Delta r_{AS^o} = -k_{A \to AS^o} C_A a_{S^o} \left(\frac{V_r}{S^o}\right) \eta_{S^o AS^o} + k_{AS^o \to A} C_{AS^o} \eta_{S^o AS^o} + k_{AS^o \to AS^*} C_{AS^o} a_{S^*} \eta_{S^o AS^o} - -k_{P \to PS^o} C_P a_{S^o} \left(\frac{V_r}{S^o}\right) \eta_{S^o PS^o} \xi_{P \to PS^o} + k_{PS^o \to P} C_{PS^o} \eta_{S^o PS^o} \qquad \left[\left(\frac{m_{S^o avb}^2}{m_{S^o tot}^2}\right) \frac{1}{s}\right] \tag{26}$$

$$\Delta r_{AS^*} = -k_{A \to AS^*} C_{AS^o} a_{S^*} \left(\frac{S^o}{S^*}\right) \eta_{S^* AS^*} \xi_{A \to AS^*} + k_{PS^* \to P} C_{PS^*} \eta_{S^* PS^*} - -k_{A \to AS^*} C_A a_{S^*} \left(\frac{V_r}{S^*}\right) \eta_{S^* AS^*} \xi_{A \to AS^*} \qquad \left[\left(\frac{m_{S^* avb}^2}{m_{S^* tot}^2}\right) \frac{1}{s}\right] \tag{27}$$

Notice that in the above equations a_{S^o} and a_{S^*} represent the normalized (active and inactive) catalyst surface available for the reaction process. These surfaces are considered as *reactant species*, and they have units $(m_{S^o available}^2/m_{S^o total}^2)$ and $(m_{S^* available}^2/m_{S^* total}^2)$, respectively.

As mentioned above, two main process variables, the volumetric concentrations of reactant C_A and product C_P only appear in the free-flowing stream in the reactor, therefore in the main physical domain defined by $x \in [0, L]$ & $y \in [-H, H]$ (Eqs. (18) and (19)). All other species and their process variable representations appear in Eqs. (20) through (27). These are the surface concentrations of reactant and product C_{AS^o}, C_{AS^*}, C_{PS^*}, C_{PS^o}, as well as the available inactive and active catalyst surfaces, a_{S^o} and a_{S^*} Clearly, these surface species reside only in the physical domain$x \in [0, L]$ @ $y = -H$ & @ $y = H$, which is placed on both boundaries.

Using the user-defined scaling parameters one can determine the Characteristic Times for each elemental step represented in

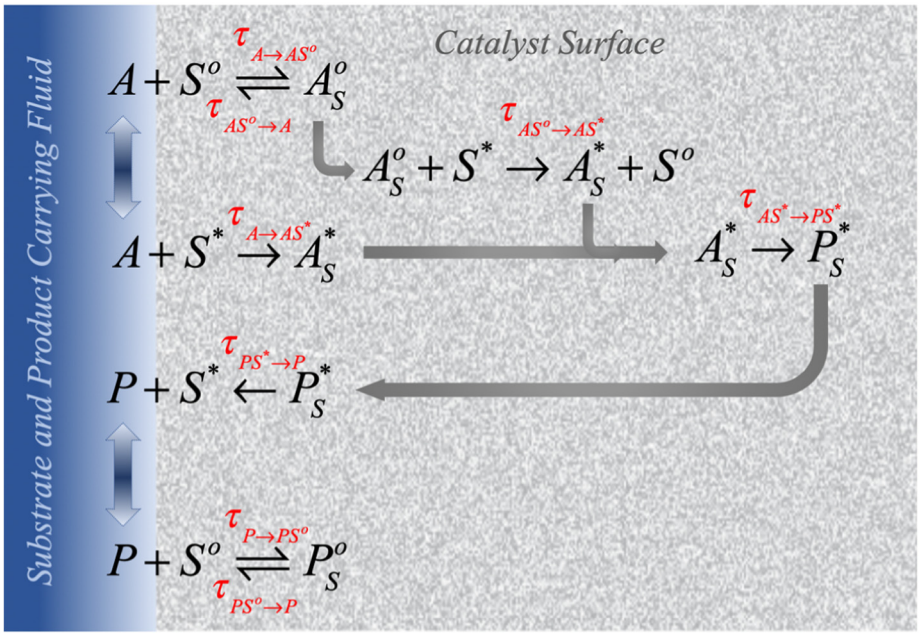

Fig. 5. Schematic representation of elementary stoichiometric reaction steps in a solid catalyzed reaction with involved Characteristic Times of kinetics elemental steps.

the mathematical model and depicted in Fig. 4. Eqs. (18), (18a), (19) and (19a) yield the characteristic times similarly to what was developed in the Eqs. (16) and (17).

Here is demonstrated the development of characteristic times for the boundary condition that connects the "two" physical domains: the diffusion rate of species *A* to the catalyst surface at the boundary of the main domain, and the reaction kinetic events at the catalyst surface.

Rewritten second boundary condition in Eq. (18a) in completed form:

$$-D_A A_n \left.\frac{\partial C_A}{\partial y}\right|_{y=H} = V_r\left(\Delta r_{C_A}\right) = V_r\left(\begin{array}{c} -k_{A\to AS^o} C_A a_{S^o} + k_{AS^o\to A} C_{AS^o}\left(\frac{S^o}{V_r}\right)\xi_{A\to AS^o} - \\ -k_{A\to AS^*} C_A a_{S^*} \end{array}\right) \quad (18b)$$

Again, the scaled variables could be represented as,

$$C_A^* = \frac{C_A}{C_{Ain}};\ C_{AS^o}^* = \frac{C_{AS^o}\left(\frac{S^o}{V_r}\right)\xi_{A\to AS^o}}{C_{Ain}};\ y^* = \frac{y}{H}$$

Note that a_{S^o} and a_{S^*} were already scaled as they were initially represented in the elemental kinetic expressions.

After substitutions, the boundary condition in Eq. (18b) converts into:

$$D_A A_n \frac{1}{(A_n H)} \frac{\partial C_A^*[1,x] C_{Ain}}{\partial y^*} \frac{1}{H} = k_{A\to AS^o} C_A^*[1,x] C_{Ain} a_{S^o} + \\ + k_{A\to AS^*} C_A^*[1,x] C_{Ain} a_{S^*} - \\ -k_{AS^o\to A} C_{AS^o}^* C_{Ain}\left(\frac{V_r}{S^o}\right)\left(\frac{S^o}{V_r}\right)\frac{\xi_{A\to AS^o}}{\xi_{A\to AS^o}} \quad (18c)$$

And, after simple algebraic manipulations we can obtain,

$$\frac{D_A}{H^2}\frac{\partial C_A^*}{\partial y^*} = k_{A\to AS^o} C_A^* a_{S^o} - k_{AS^o\to A} C_{AS^o}^* + k_{A\to AS^*} C_A^* a_{S^*} \quad (18d)$$

The coefficients in the normalized Equation (18d) represent the characteristic times.

$$\frac{1}{\tau_{diff_y}}\frac{\partial C_A^*}{\partial y^*} = \frac{1}{\tau_{A\to AS^o}} C_A^* a_{S^o} - \frac{1}{\tau_{AS^o\to A}} C_{AS^o}^* + \frac{1}{\tau_{A\to AS^*}} C_A^* a_{S^*} \quad (18e)$$

All Characteristic Times, pertinent for this solid catalyzed process illustrated in Figs. 4 and 5, are given in Table 2.

Again, a simple time scale analysis approach could provide insight into potentially critical rate steps in the overall chemical reaction process scheme. For example, one can now easily relate the characteristic times arising from transport mechanisms (τ_{diff_y-A}; τ_{diff_y-P}; τ_{diff_x-A}; τ_{diff_x-P}; τ_{mrt}) with the rest of the characteristic times in Table 2 arising from elemental kinetic steps. However, one should notice that most of the kinetic steps in the envisioned catalysis scheme are transport steps – see illustration in Fig. 4 (b, c, d, and f). The only exception is the 4e step, which is a true chemical conversion step. Nevertheless, there are compelling reasons to believe that all adsorption/desorption steps and surface diffusion steps could be successfully described as Arrhenius type processes. (Bosworth, 1956; Lennard-Jones, 1932).

Once all the characteristic times are defined, one could outline the challenge of determining the best line-up of the values of the characteristic times involved. As the first step in this process, one should define an objective function to be improved, reduced, or increased, which should be expressed in terms of characteristic

Table 2
The Characteristic Times relevant to the solid catalyzed process shown in Figs. 4 and 5.

τ_{diff_y-A}	τ_{diff_y-P}	τ_{diff_x-A}	τ_{mrt}	$\tau_{A\to AS^o}$	$\tau_{AS^o\to A}$
$\frac{H^2}{D_A}$	$\frac{H^2}{D_P}$	$\frac{L^2}{D_A}$	$\frac{L}{u_x}=\frac{V_r}{F}$	$\frac{1}{k_{A\to AS^o}}$	$\frac{1}{k_{AS^o\to A}}$
$\tau_{A\to AS^*}$	$\tau_{AS^o\to AS^*}$	$\tau_{AS^*\to PS^*}$	$\tau_{PS^*\to P}$	$\tau_{P\to PS^o}$	$\tau_{PS^o\to P}$
$\frac{1}{k_{A\to AS^*}}$	$\frac{1}{k_{AS^o\to AS^*}}$	$\frac{1}{k_{AS^*\to PS^*}}$	$\frac{1}{k_{PS^*\to P}}$	$\frac{1}{k_{P\to PS^o}}$	$\frac{1}{k_{PS^o\to P}}$

times. The operating parameters, which are realistically available for an easy engineering intervention and adjustment of the values of the characteristic times, are: H, L, F, T, S^o, and S^*. The parametric exploration of operating parameters, which would yield a set of parameters that improves the objective function, may require a formalized search process and all pertinent constraints. A collateral benefit of the parametric exploration is the identification of certain characteristic times that need the most extensive adjustments to facilitate process improvement. Therefore, we are enabled to discover where the points of process intensification are required, and which parameters are at our disposal to accomplish the change. Then, it is only up-to engineering ingenuity to conceive the innovative design solutions, which would be aligned with the better choice of parameters and more fitting values of characteristic times.

In Part II of this paper, we briefly discuss the innovative opportunities as they are related to the process intensification and general "improvement" of the process flow sheet.

5. Conclusions

In this work we illustrated the formation of Characteristic Times and the Time-Scale Analysis in the design of a solid catalyzed reaction process and presented several important outcomes.

First, an encompassing, comprehensive definition of Characteristic Times and its use in characterizing transport phenomena and reaction kinetics in microstructured architecture was presented with *Characteristic Times* enabling observation and understanding of intricate details of chemical reaction processes.

Additionally, the origin of Characteristic Times was traced to fundamental processes such as the kinetic theory of diffusion and Arrhenius-type kinetics which clearly demonstrated that these fundamental phenomena, when imbedded into the first principle equations (i.e. mass, energy and momentum balance, etc.), will yield Characteristic Times for every element of the balance equation.

Lastly and equally important, it was shown that the user must make intelligent choices, through a process known as equation scaling, to edify specific parts of the processes by selecting reasonable and self-examining scaling parameters.

CRediT authorship contribution statement

Goran N. Jovanovic: Conceptualization, Methodology, Writing - review & editing. **Matthew Y. Coblyn:** Conceptualization, Methodology, Writing - review & editing. **Igor Plazl:** Conceptualization, Methodology, Writing - review & editing.

Declaration of Competing Interest

The authors declare that they have no known competing financial interests or personal relationships that could have appeared to influence the work reported in this paper.

Acknowledgements

We gratefully acknowledge the financial support from "Modular Chemical Process Intensification 'BOOT CAMP'" RAPID Education & Workforce Development Project (Award No DE-EE0007888-3.2.3). Which catalyzed the development of the Time Scale Analysis technical approach. The financial support of the Slovenian Research Agency through Grant P2-0191, and projects J7-1816, J4-1775, BI-Fr/19-20 Proteus 007 and N2-0067 is acknowledged.

References

Bieringer, T., Buchholz, S., Kockmann, N., 2013. Future production concepts in the chemical industry: modular – small-scale – continuous. Chem. Eng. Technol. 36, 900–910. https://doi.org/10.1002/ceat.201200631.

Bosworth, R.C.L., 1956. Transport Processes in Applied Chemistry: The Flow of Physical Properties in Chemical Reactors. Wiley.

Carr, E.J., 2018. Characteristic time scales for diffusion processes through layers and across interfaces. Phys. Rev. E 97,. https://doi.org/10.1103/PhysRevE.97.042115 042115.

Caudal, J., Fiorina, B., Massot, M., Labégorre, B., Darabiha, N., Gicquel, O., 2013. Characteristic chemical time scales identification in reactive flows. Proc. Combust. Inst. 34, 1357–1364. https://doi.org/10.1016/j.proci.2012.06.178.

Chávez, F., Debenedetti, P.G., Luo, J.J., Dave, R.N., Pfeffer, R., 2003. Estimation of the Characteristic Time Scales in the Supercritical Antisolvent Process. Ind. Eng. Chem. Res. 42, 3156–3162. https://doi.org/10.1021/ie021048j.

Einstein, A., 1956. Investigations on the Theory of the Brownian Movement. Courier Corporation.

Fogler, H.S., 2006. Elements of Chemical Reaction Engineering, 4th edition. Prentice Hall PTR, New Jersey.

Gupta, R., Fletcher, D.F., Haynes, B.S., 2010. Taylor flow in microchannels: a review of experimental and computational work. J. Computat. Multiphase Flows 2, 1–31. https://doi.org/10.1260/1757-482X.2.1.1.

Henze, M., van Loosdrecht, M.C.M., Ekama, G.A., Brdjanovic, D., 2008. Biological Wastewater Treatment. IWA Publishing, London.

Hunter, S.M., Susanne, F., Whitten, R., Hartwig, T., Schilling, M., 2018. Process design methodology for organometallic chemistry in continuous flow systems. Tetrahedron, Eng. Chem. Future Organic Synthesis 74, 3176–3182. https://doi.org/10.1016/j.tet.2018.04.020.

Isaac, B.J., Parente, A., Galletti, C., Thornock, J.N., Smith, P.J., Tognotti, L., 2013. A novel methodology for chemical time scale evaluation with detailed chemical reaction kinetics. Energy Fuels 27, 2255–2265. https://doi.org/10.1021/ef301961x.

Isvoranu, D., Dănăilă, S., Bogoi, A., Levenţiu, C., 2018. Assessment of chemical time scale for a turbine burner. Transport. Res. Procedia, Aerospace Europe CEAS 2017 Conference 29, 181–190. https://doi.org/10.1016/j.trpro.2018.02.016.

Kim, Y.-H., Park, L.K., Yiacoumi, S., Tsouris, C., 2017. Modular chemical process intensification: a review. Annu. Rev. Chem. Biomol. Eng. 8, 359–380. https://doi.org/10.1146/annurev-chembioeng-060816-101354.

Klinke, D.J., Finley, S.D., 2012. Timescale analysis of rule-based biochemical reaction networks. Biotechnol. Progress 28, 33–44. https://doi.org/10.1002/btpr.704.

Lennard-Jones, J.E., 1932. Processes of adsorption and diffusion on solid surfaces. Trans. Faraday Soc. 28, 333–359. https://doi.org/10.1039/TF9322800333.

Lev, O., Regli, S., 1992. Evaluation of ozone disinfection systems: characteristic time *T*. J. Environ. Eng. 118, 268–285. https://doi.org/10.1061/(ASCE)0733-9372(1992)118:2(268).

Li, X., Dai, Z., Wang, F., 2017. Characteristic chemical time scale analysis of a partial oxidation flame in hot syngas coflow. Energy Fuels 31, 4382–4390. https://doi.org/10.1021/acs.energyfuels.6b02490.

Maas, U., Pope, S.B., 1992. Simplifying chemical kinetics: Intrinsic low-dimensional manifolds in composition space. Combust. Flame 88, 239–264. https://doi.org/10.1016/0010-2180(92)90034-M.

Marques, M.P.C., Fernandes, P., 2011. Microfluidic devices: useful tools for bioprocess intensification. Molecules 16, 8368–8401. https://doi.org/10.3390/molecules16108368.

Miložič, N., Lubej, M., Lakner, M., Žnidaršič-Plazl, P., Plazl, I., 2017. Theoretical and experimental study of enzyme kinetics in a microreactor system with surface-immobilized biocatalyst. Chem. Eng. J. 313, 374–381. https://doi.org/10.1016/j.cej.2016.12.030.

Pohar, A., Plazl, I., 2009. Process intensification through microreactor application. Chem. Biochem. Eng. Q. 23, 537–544.

Šalić, A., Zelić, B., 2018. Synergy of microtechnology and biotechnology: microreactors as an effective tool for biotransformation processes§: §The paper was presented at European Biotechnology Congress, 25–27 May 2017, Dubrovnik, Croatia. Food Technol. Biotechnol. 56, 464–479. https://doi.org/10.17113/ftb.56.04.18.5673.

Seifert, T., Sievers, S., Bramsiepe, C., Schembecker, G., 2012. Small scale, modular and continuous: A new approach in plant design. Chem. Eng. Process. Process Intensif. 52, 140–150. https://doi.org/10.1016/j.cep.2011.10.007.

Stankiewicz, A.I., Moulijn, J.A., 2000. Process intensification: transforming chemical engineering. Chem. Eng. Prog. 96 (1), 22–34.

Wartha, E.-M., Bösenhofer, M., Harasek, M., 2020. Characteristic chemical time scales for reactive flow modeling. Combust. Sci. Technol., 1–26 https://doi.org/10.1080/00102202.2020.1760257.

Wegeng, R.S., Drost, M.K., Brenchley, D.L., 2000. Process intensification through miniaturization of chemical and thermal systems in the 21st Century. In: Ehrfeld, W. (Ed.), Microreaction Technology: Industrial Prospects. Springer, Berlin, Heidelberg, pp. 2–13. https://doi.org/10.1007/978-3-642-59738-1_1.

Wohlgemuth, R., Plazl, I., Žnidaršič-Plazl, P., Gernaey, K.V., Woodley, J.M., 2015. Microscale technology and biocatalytic processes: opportunities and challenges for synthesis. Trends Biotechnol. 33, 302–314. https://doi.org/10.1016/j.tibtech.2015.02.010.

Yoshida, J., Nagaki, A., Iwasaki, T., Suga, S., 2005. Enhancement of chemical selectivity by microreactors. Chem. Eng. Technol. 28, 259–266. https://doi.org/10.1002/ceat.200407127.